



Working Gases for Beam Induced Fluorescence at the CERN e-Lens

S. Udrea, P. Forck, D. Vilsmeier

GSI Helmholtzzentrum für Schwerionenforschung, Darmstadt, Germany

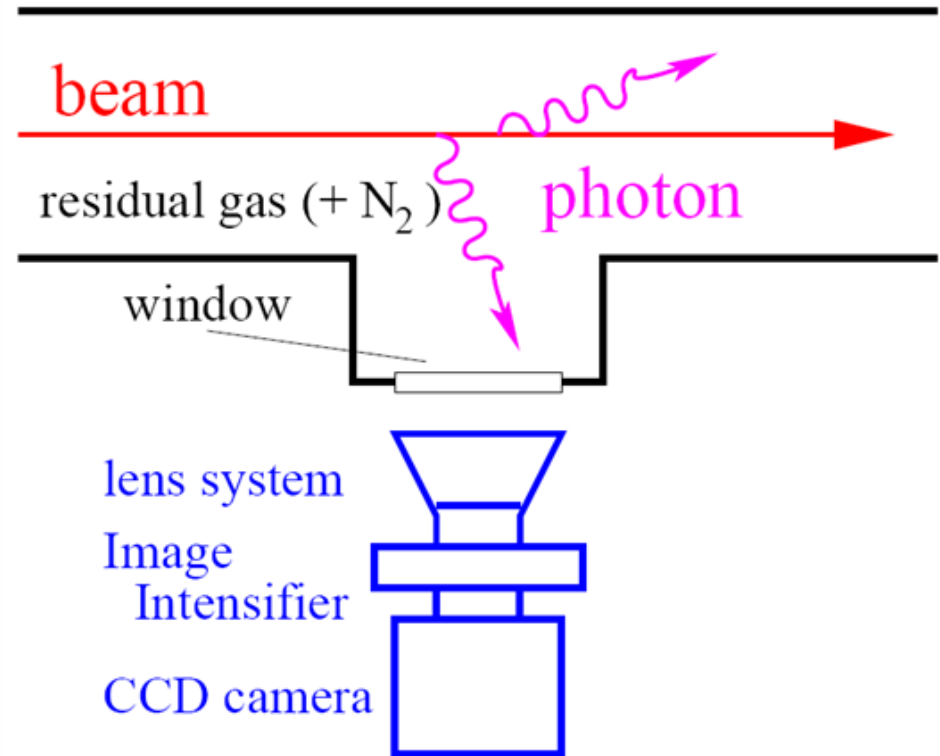


- Beam Induced Fluorescence (BIF) working principle and features
- Characteristics of the CERN e-lens setup
- N_2 , Ne and Ar as working gases
- Image distortion due to electromagnetic fields
- Curtain thickness influence
- Possible show stoppers
- Conclusion

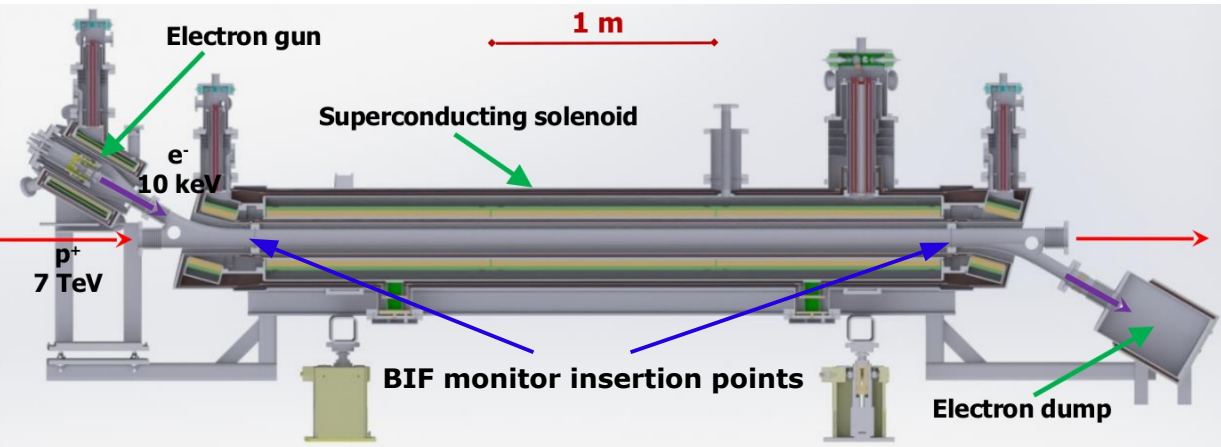
Beam Induced Fluorescence (BIF)



- Based upon the detection of photons emitted by residual or injected (low pressure) gas molecules
- Little influence on the beam
- Single pulse observation possible; e.g. $\approx 1 \mu\text{s}$ time resolution (depends on photon flux)
- Spatial resolution can be matched to application
- In case of low photon fluxes, commercial intensified cameras are available
- Compact installation, e.g. 25 cm for both planes



E-Lens and BIF @ CERN



Longitudinal cross section through the planned electron lens, see: Diego Perini, Carlo Zanoni, *Preliminary Design Study of the Hollow Electron Lens for LHC*, arxiv.org/abs/1702.00234

Hollow e^- beam, 5 A, 10 keV, 10.5 mm outer and 7 mm inner diameter

p^+ beam, 1.1 A, 7 TeV, 0.83 mm FWHM diameter

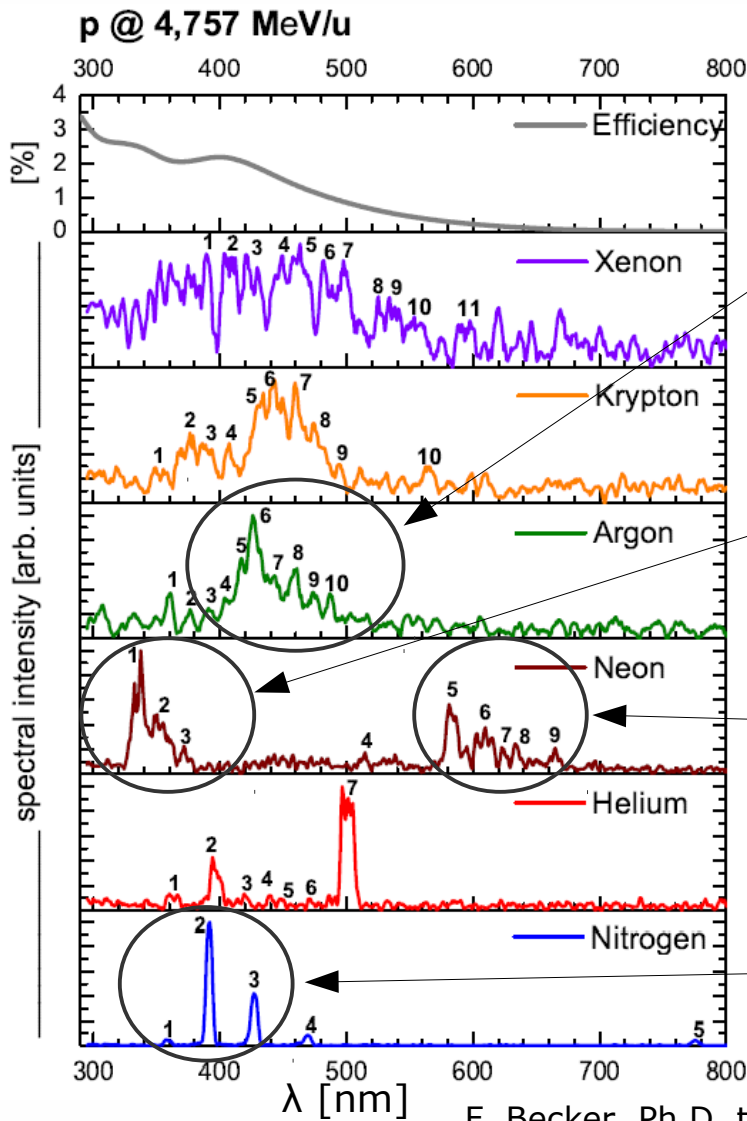


Gas jet curtain (gas molecules move into slide surface)

<4 T longitudinal magnetic field

Sketch not to scale!

Fluorescence of different gases



Strongest emission from Ar^+ blue/green lines mainly corresponding to different $[3s^2 3p^4(^3P)] 4p \rightarrow 4s$ transitions with life times of 10-20 ns.

Several Ne^+ UV lines mainly corresponding to different $[2s^2 2p^4(^3P)] 3p \rightarrow 3s$ transitions with life times below 10 ns.

Several Ne yellow/red lines mainly corresponding to different $[2s^2 2p^5(^2P)] 3p \rightarrow 3s$ transitions with life times of about 20 ns.

The strong UV/blue lines correspond to the $B^2\Sigma_u^+ \rightarrow X^2\Sigma_g^+$ electronic transition band of N_2^+ , life times are of about 60 ns.

F. Becker, Ph.D. thesis, T.U. Darmstadt, Germany, 2009

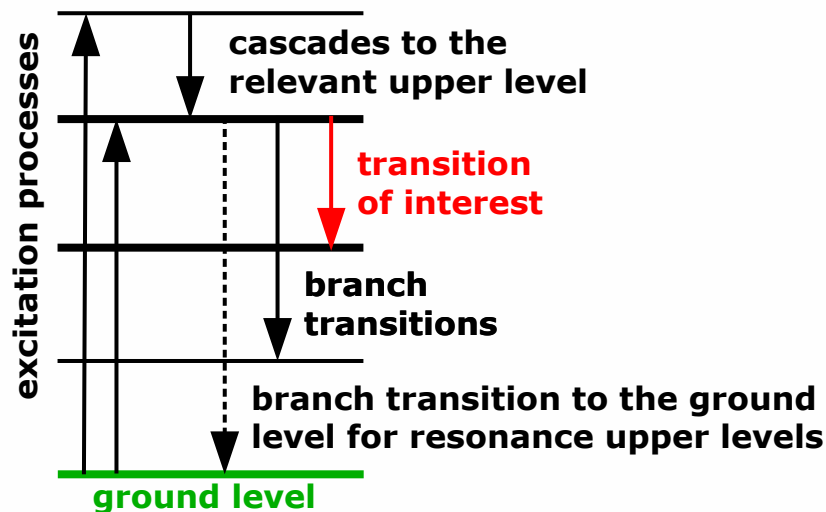
Warning on cross sections



emission* cross section \neq excitation cross section

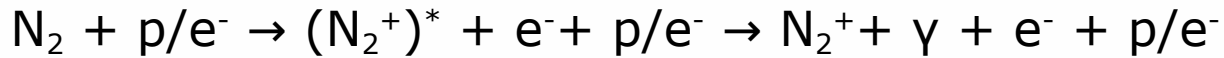
Emission cross sections are relevant for BIF diagnostics and may be affected by cascades – the upper level of the observed transition gets populated from higher excited levels – and pressure – attention has to be paid both to the working pressure and the pressure for which data is available. Moreover the experimental setup's geometry may play an important role.

Excitation cross sections are not directly relevant for BIF diagnostics. However, theoretical models usually target these cross sections, which may be used to estimate the emission cross sections by taking branching into account and an appropriate modeling of cascades and pressure effects.



(*) also known as fluorescence cross section

N₂ as working gas: excitation and emission



Leads to the electronic transition $\text{B}^2\Sigma_u^+ \rightarrow \text{X}^2\Sigma_g^+$ of the molecular ion with wavelengths around 391 nm, depending upon involved vibrational and rotational states. **Remark: cross section data available for a broad range of energies, up to p@450 GeV!**

ν' (upper level)	ν'' (lower level)	λ [nm]
1	0	358.2
0	0	391.4
0	1	427.8

strongest line



Drives the electronic transition $\text{C}^3\Pi_u \rightarrow \text{B}^3\Pi_g$ of the neutral molecule with wavelengths around 337 nm. This process cannot be initiated directly by protons because it implies a spin flip mechanism: the upper $\text{C}^3\Pi_u$ state is a triplet one, while the ground state of N_2 is a singlet and total spin should stay preserved during excitation. **Remark: presently cross section data available just at low energies for e⁻ impact!**

ν' (upper level)	ν'' (lower level)	λ [nm]
1	0	315.9
0	0	337.1
0	1	357.7

strongest line

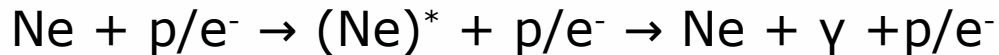
Ne as working gas: excitation and emission



Leads to several $[2s^22p^4(^3P)]3p \rightarrow 3s$ transitions of the Ne^+ ion with wavelengths between 300 and 400 nm. All transitions in the table below have lifetimes of about 6 ns. **Remark: No cross section data identified until now!**

$[2s^22p^4(^3P)]3p$	$[2s^22p^4(^3P)]3s$	λ [nm]
J=7/2	J=5/2	319.9
J=3/2	J=3/2	332.4
J=1/2	J=1/2	337.8

strongest line

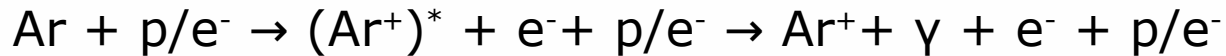


Drives several $[2s^22p^5(^2P)]3p \rightarrow 3s$ transitions of Ne with wavelengths above 580 nm. Available data from the literature strongly suggests that the by far strongest line is due to the $2p_1 \rightarrow 1s_2$ (Paschen notation) transition at 585.4 nm. The upper level has a lifetime of about 15 ns. **Remark: Cross section data just at low energies until now! Cascades are expected to have little contribution to populating the $2p_1$ level.**

$[2s^22p^5(^2P)]3p$	$[2s^22p^5(^2P)]3s$	λ [nm]
$2p_1$	$1s_2$	585.4
$2p_3$	$1s_4$	607.4
$2p_6$	$1s_5$	614.3

strongest line

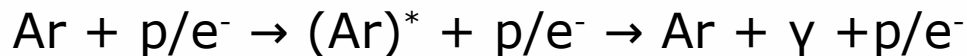
Ar as working gas: excitation and emission



Leads to several $[3s^23p^4(^3P)]4p \rightarrow 4s$ transitions of the Ar^+ ion with wavelengths between 400 and 500 nm. All transitions in the table below have lifetimes of 10-20 ns. **Remark: presently cross section data available just at low energies for e^- impact! Upper levels are also populated by cascades \Rightarrow emission delays higher than indicated by lifetimes.**

$[3s^23p^4(^3P)]4p$	$[2s^22p^4(^3P)]4s$	λ [nm]
$^2P^o_{3/2}$	$^2D_{5/2}$	427.8
$^2F^o_{7/2}$	$^2D_{5/2}$	461.0
$^2P^o_{3/2}$	$^2P_{1/2}$	476.5

strongest line

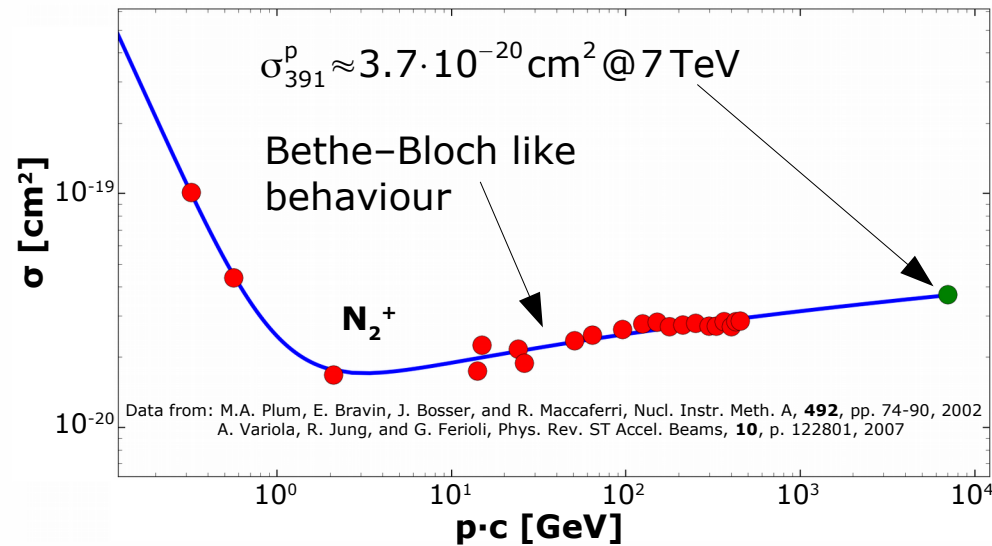
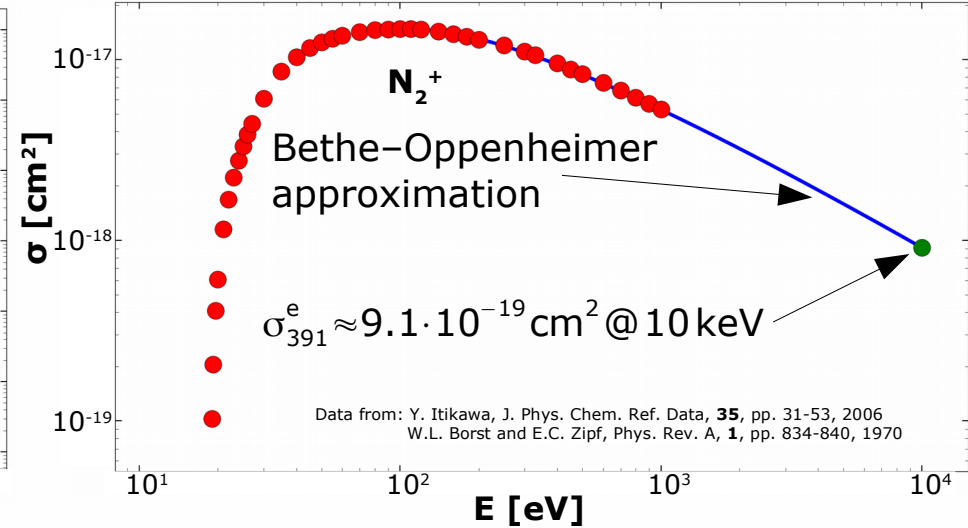
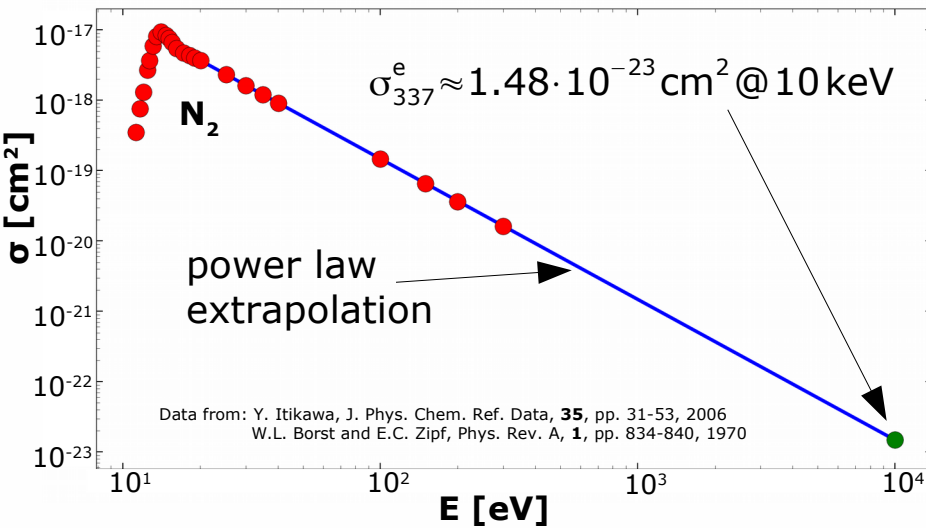


Drives several $[3s^23p^5(^2P)]4p \rightarrow 4s$ transitions of Ar with the strongest at wavelengths above 700 nm. The upper levels from the table have lifetimes of 20-40 ns. **Remark: presently cross section data available just at low energies for e^- impact! Upper levels are also populated by cascades \Rightarrow emission delays higher than indicated by lifetimes.**

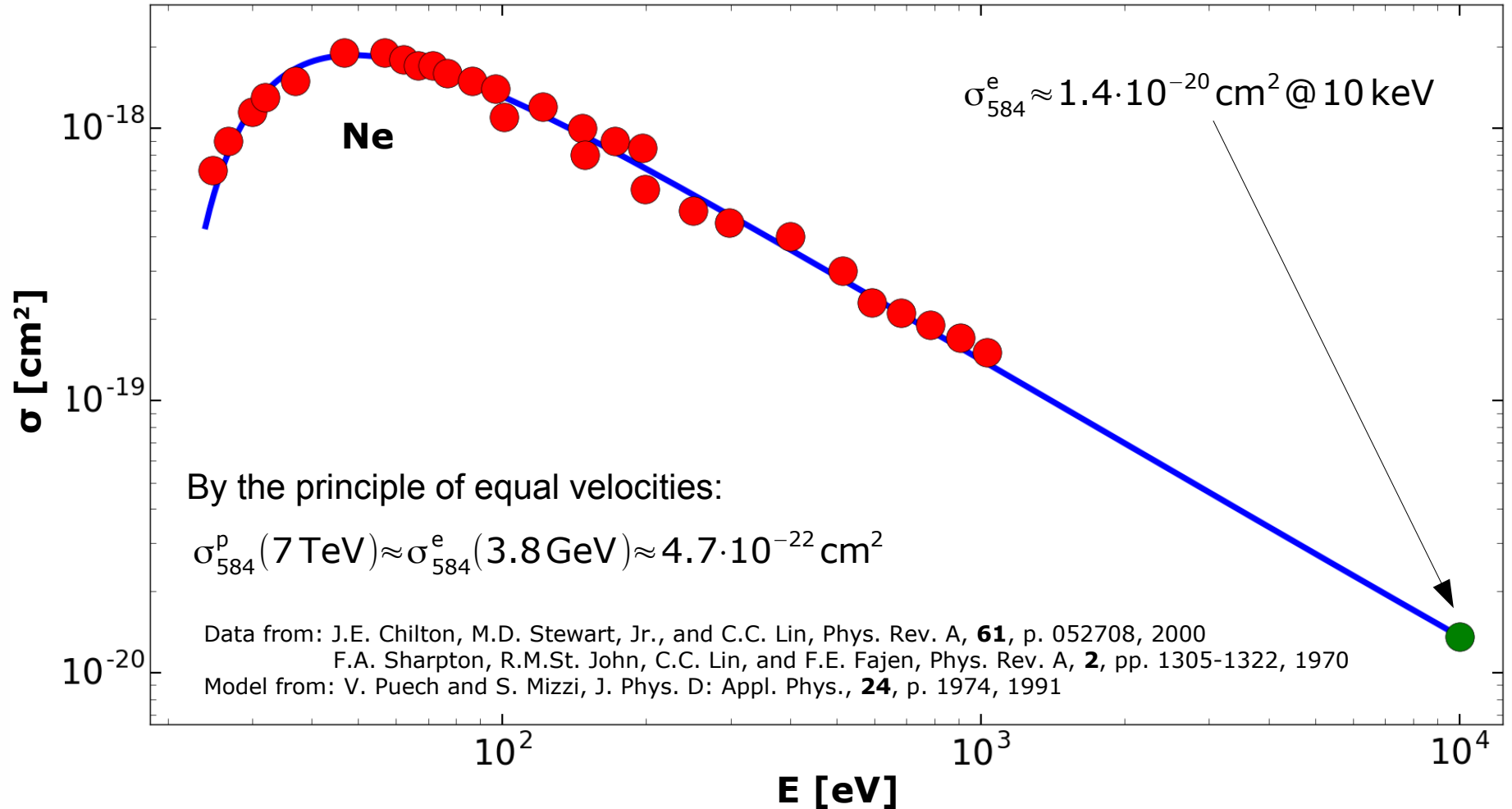
$[3s^23p^5(^2P)]4p$	$[3s^23p^5(^2P)]4s$	λ [nm]
$2p_1$	$1s_2$	750.4
$2p_5$	$1s_4$	751.5
$2p_7$	$1s_4$	810.4

strongest line

N₂ as working gas: cross sections



Ne as working gas: cross sections



Ar as working gas: cross sections

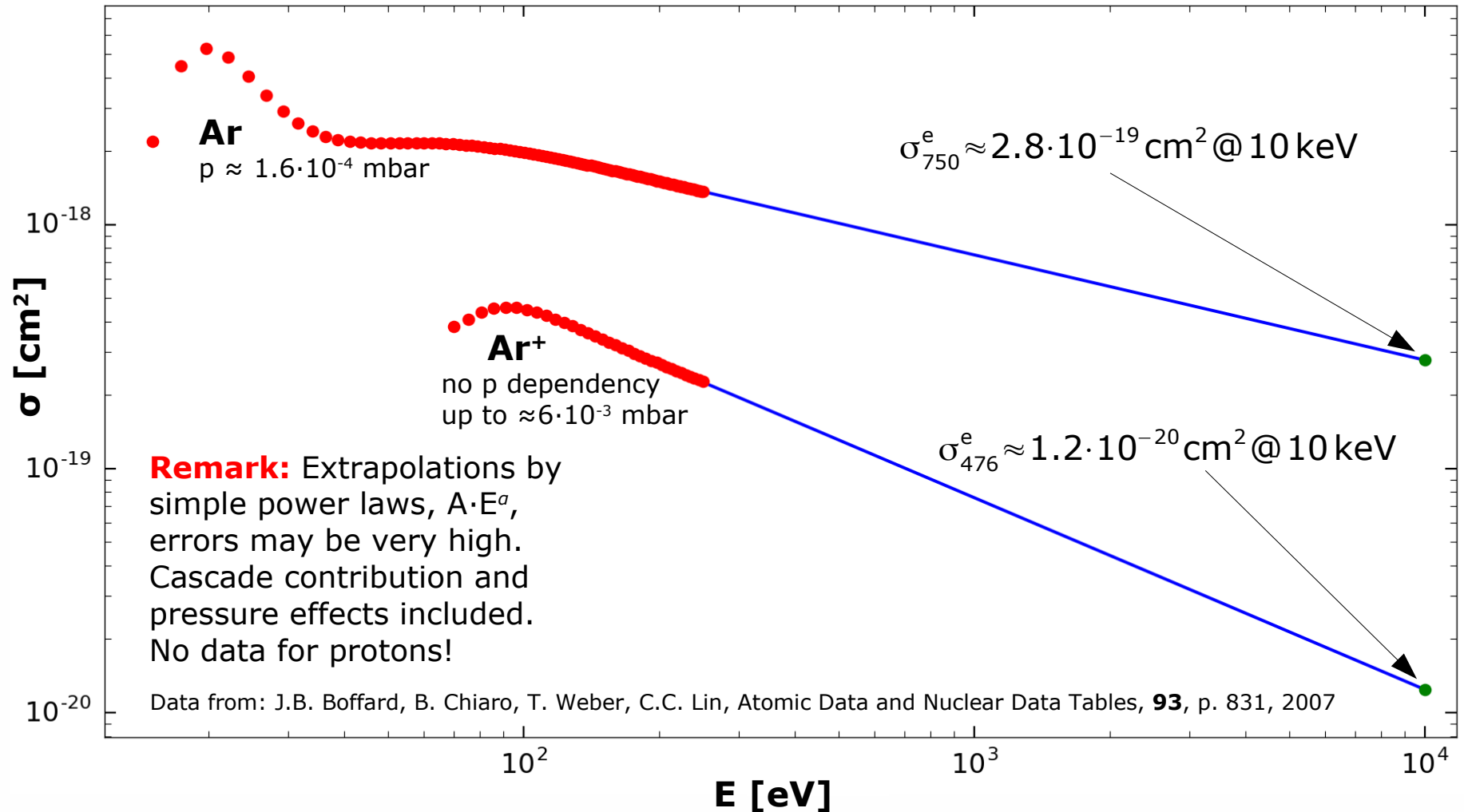


Image intensifier working principle

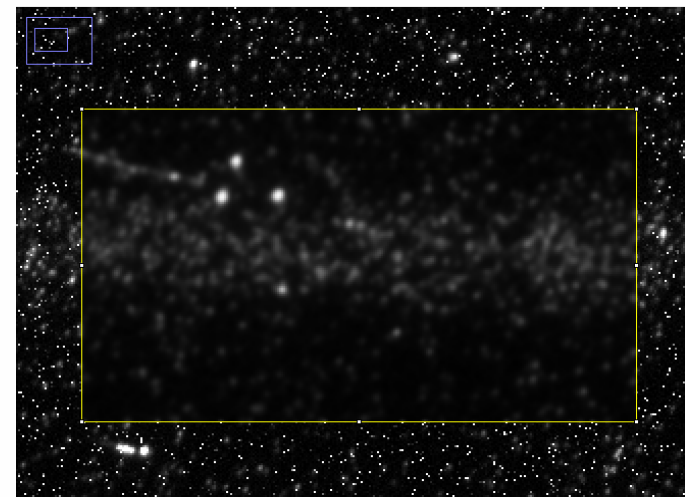
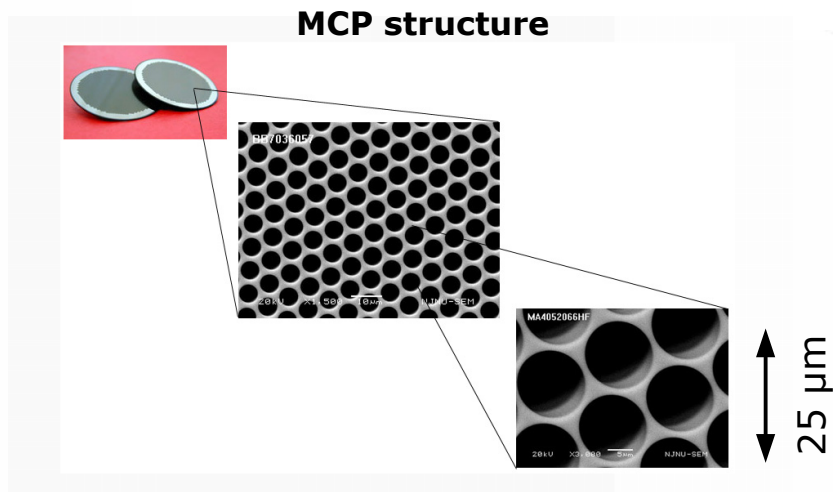
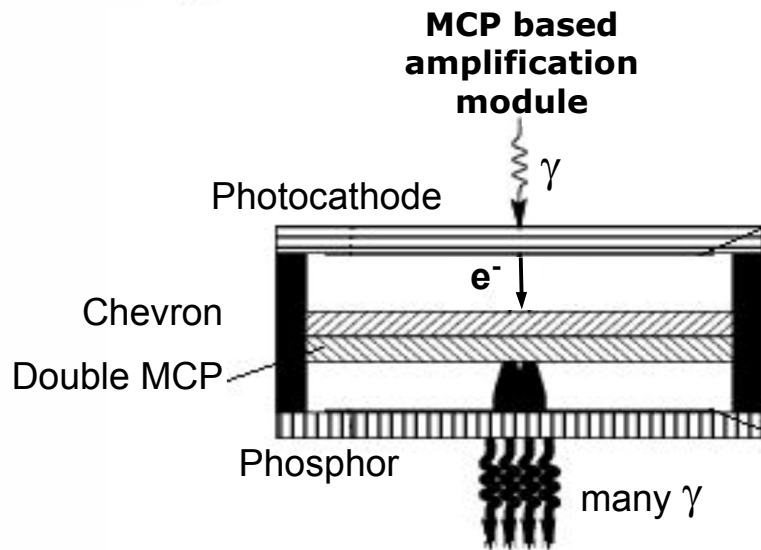


Image from $5 \cdot 10^8$, 300 MeV/u $^{238}\text{U}^{73+}$ ions in N_2 , $p = 5 \cdot 10^{-3}$ mbar.

Photocathode and camera



S20 photocathode:

- High quantum efficiency
 - Sensitive for Ne yellow line
 - Medium dark counts
 - Availability
- ⇒ UV enhanced S20 chosen

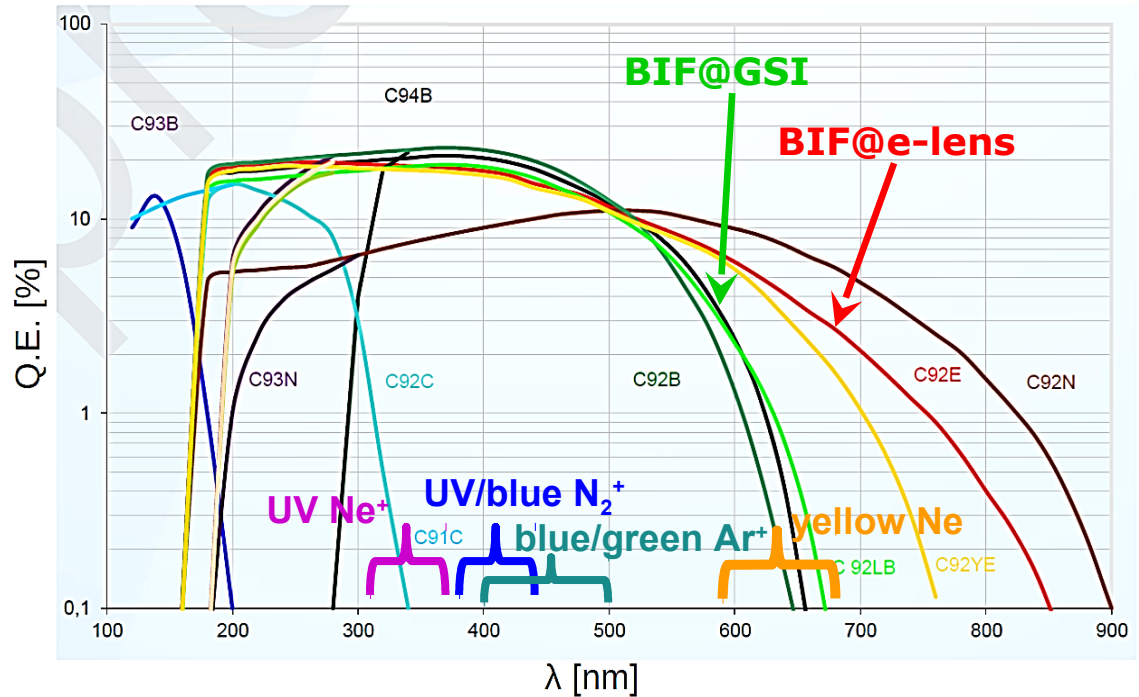


Image intensifier:

- double MCP for single photon counting;
- 10⁶ amplification

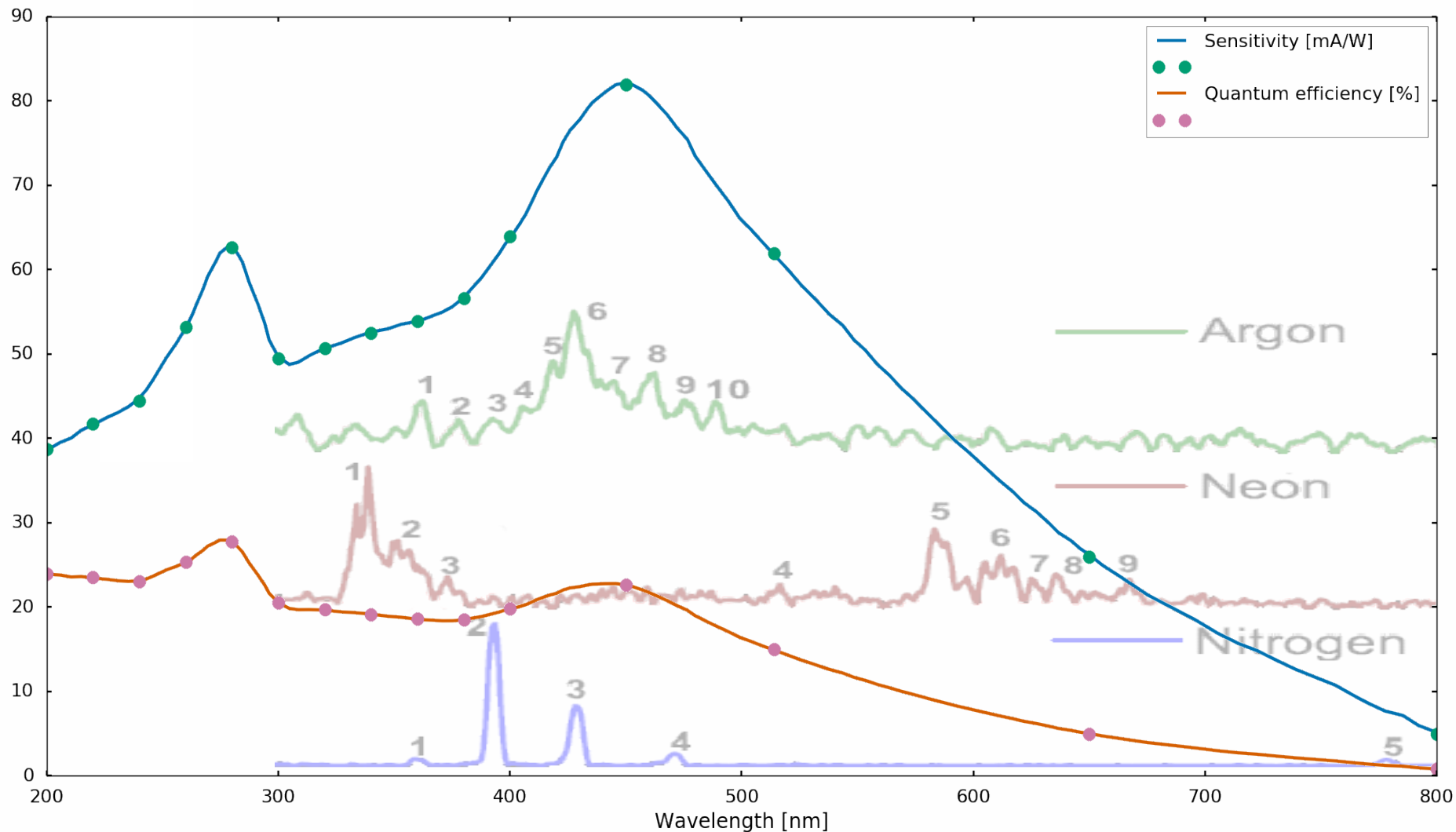
Camera:

- Simple CMOS
- Coupling to CMOS by relay optics for easy maintenance

	Designation	Material	Peak Q.E. [%]	Dark counts [1/s/cm ²]
BIF@e-lens	C92E	S20	20	600
BIF@GSI	C92LB	Low noise bialkali	20	15
	C92B, C93B, C94B	Bialkali	20	60
	C92N, C93N	S25	10	3000
	C92YE	Yellow enhanced	20	60



UV enhanced S20 spectral response



Based on data delivered by the manufacturer



Photon rate estimations



$$N_y = \sigma \cdot \frac{I \cdot \Delta t}{e} \cdot n \cdot d \cdot \frac{\Omega}{4\pi} \cdot T \cdot T_f \cdot \eta_{pc} \cdot \eta_{MCP}$$

$$n = 2.5 \cdot 10^{10} \text{ cm}^{-3} (!)$$

$$d = 5 \cdot 10^{-2} \text{ cm}$$

$$\Omega = 4\pi \cdot 10^{-4} \text{ sr}$$

$$T = 70\%$$

$$T_f = 30\%$$

$$\eta_{MCP} = 50\%$$

N_y = average number of photons detected during time Δt

σ = cross section of the photon generation process

I = electron or proton current (electrical)

e = elementary charge

n = gas density

d = distance traveled through gas (curtain thickness)

Ω = solid angle of the optics

T = transmittance of the optical system

T_f = transmittance of the optical filter

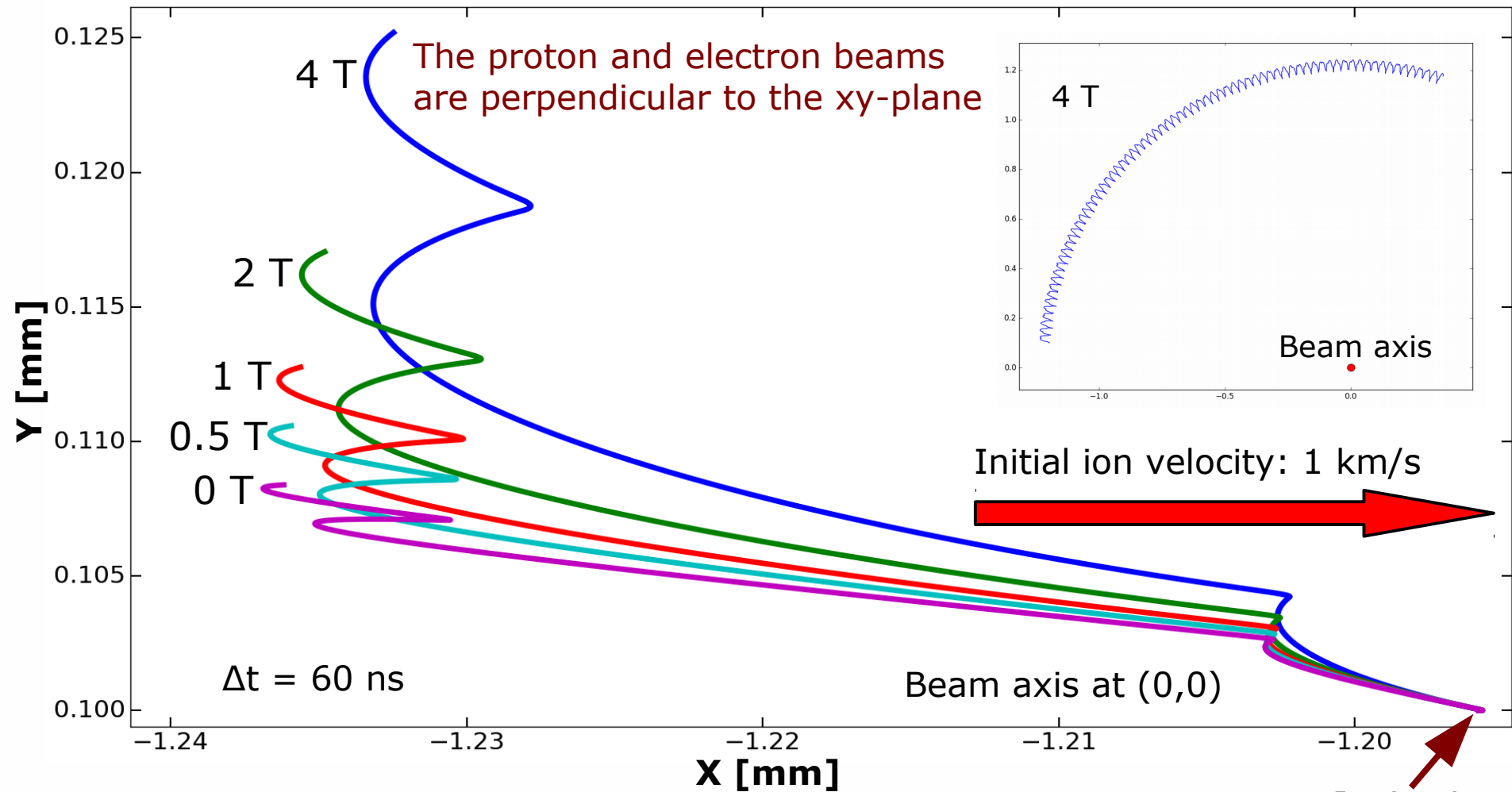
η_{pc} = quantum efficiency of the photocathode

η_{MCP} = detection efficiency of the MCP

Projectile	Emitter	λ [nm]	σ [cm ²]	I [A]	η_{pc}	N_y [s ⁻¹]	$1/N_y$ [s]
electron	N ₂	337.1	$1.5 \cdot 10^{-23}$	5	0.2	1.2	0.8
electron	N ₂ ⁺	391.4	$9.1 \cdot 10^{-19}$	5	0.2	$7.5 \cdot 10^4$	$1.3 \cdot 10^{-5}$
proton	N ₂ ⁺	391.4	$3.7 \cdot 10^{-20}$	1	0.2	$6.1 \cdot 10^2$	$1.6 \cdot 10^{-3}$
electron	Ne	585.4	$1.4 \cdot 10^{-20}$	5	0.05	$2.9 \cdot 10^2$	$3.5 \cdot 10^{-3}$
proton	Ne	585.4	$4.7 \cdot 10^{-22}$	1	0.05	1.9	0.5
electron	Ar	750.4	$2.8 \cdot 10^{-19}$	5	0.01	$1.2 \cdot 10^3$	$8.4 \cdot 10^{-4}$
electron	Ar ⁺	476.5	$1.2 \cdot 10^{-20}$	5	0.2	$9.9 \cdot 10^2$	$1.0 \cdot 10^{-3}$

Remark: The Ar⁺ cross section can be significantly increased by integrating over $400 < \lambda < 500$ nm

N_2^+ example of single particle dynamics



Remark: Initial velocity is negligible which results in a displacement $\sim (\Delta t)^2/m$ due to beam fields \Rightarrow life time is critical!



N_2^+ and Ne^+ image distortion comparison (1)

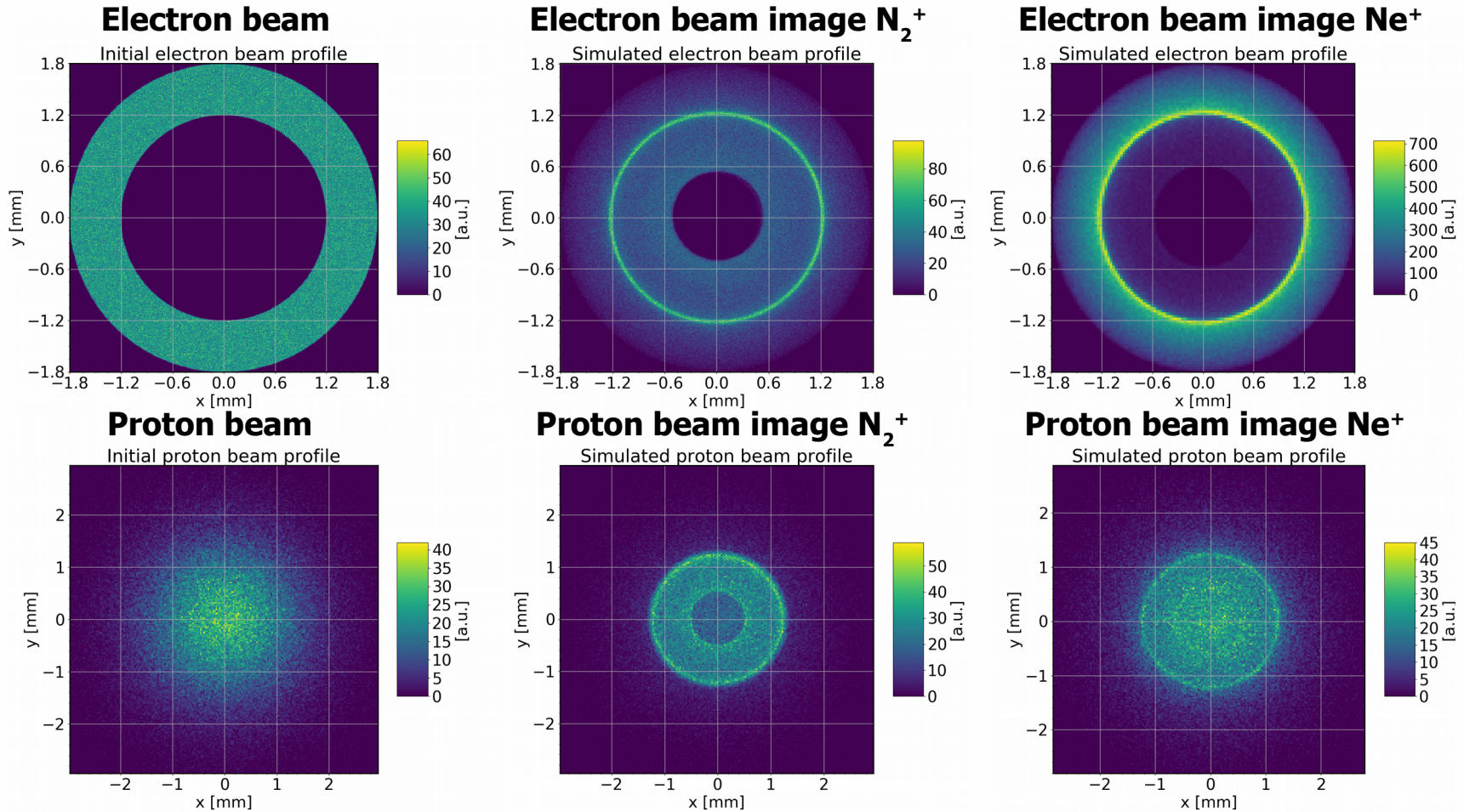


N_2^+ (blue lines): lifetime $\tau = 60$ ns , mass $m = 28$ u, $\tau^2/m \approx 129$ ns²/u

Ne^+ (UV lines): lifetime $\tau = 11$ ns* , mass $m = 20$ u, $\tau^2/m \approx 6$ ns²/u

Beams: $p \cdot 2 \cdot 10^{11}$ /bunch, $\sigma_\emptyset = 1$ mm, $\sigma_{\Delta t} = 0.6$ ns, $I_e = 5$ A (dc), $B_{sol} = 4$ T

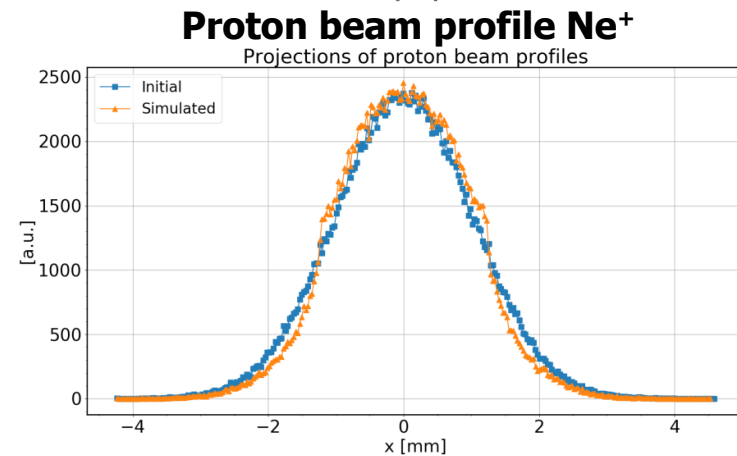
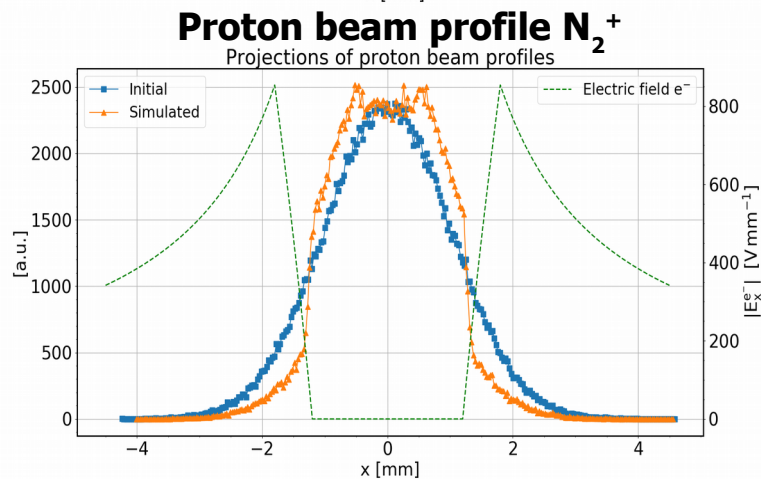
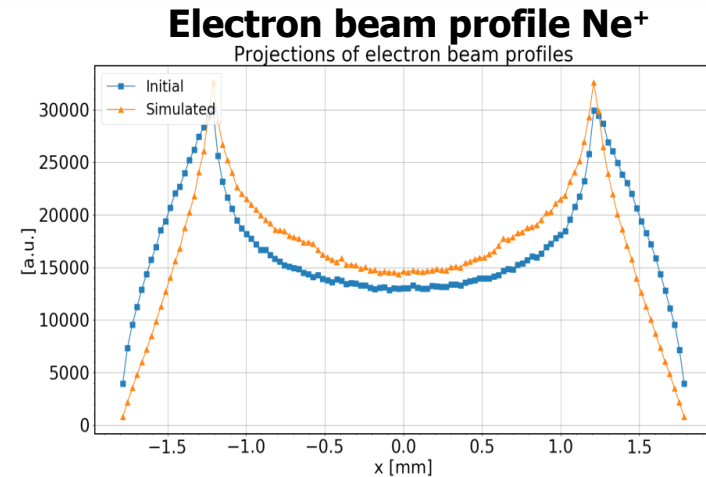
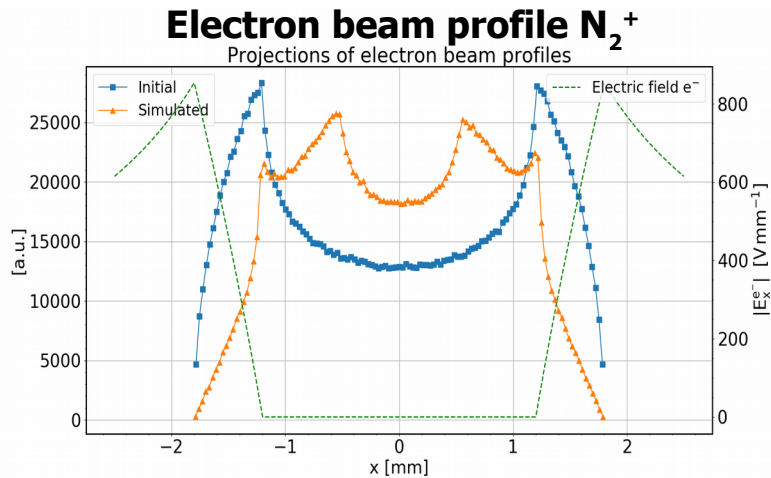
*Some cascade contribution assumed



N_2^+ and Ne^+ image distortions comparison (2)



Profiles by projection



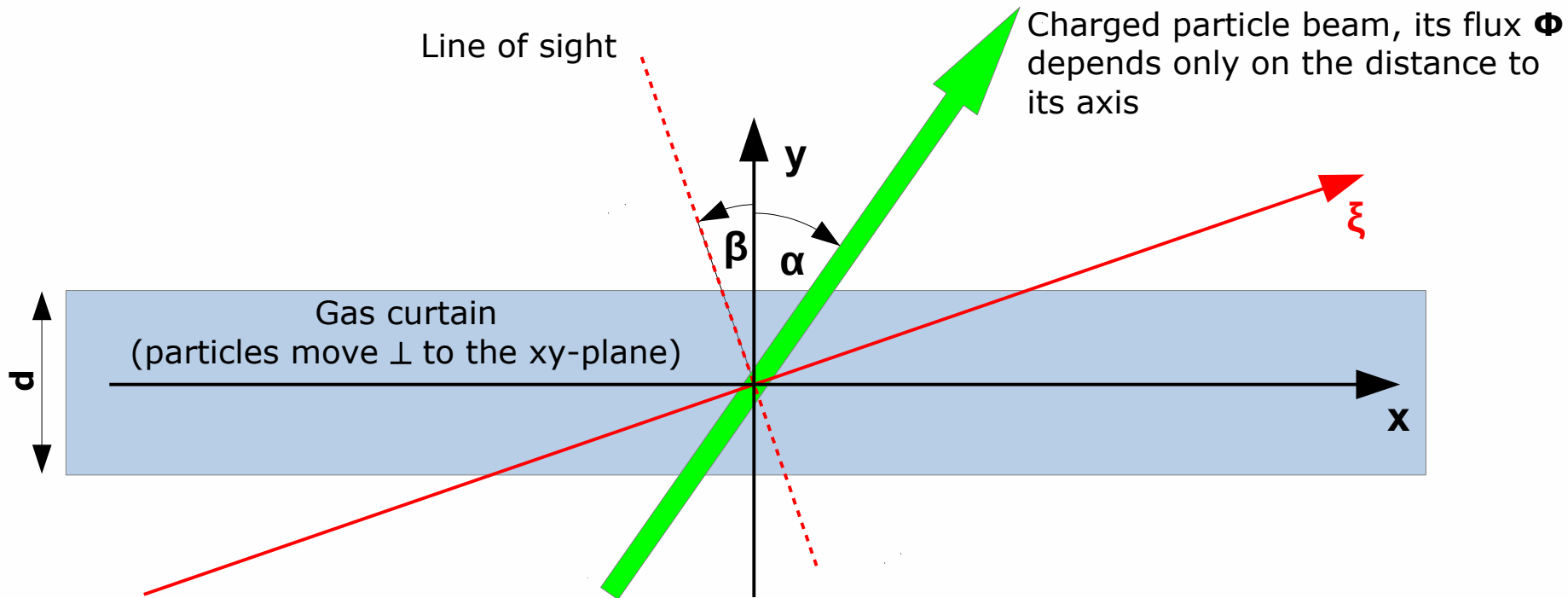
Remark: Neutral Ne (yellow lines) is not influenced by beam's space charge \Rightarrow 'ideal' working gas!

Working gases overview



	N₂	Ne	Ar
General remarks	Fluorescence almost exclusively due to N ₂ ⁺ at λ around 391 nm. Highest photon yield.	Strong fluorescence due to Ne at λ > 580 nm relatively strong emission due to Ne ⁺ .	Strong Ar lines at λ > 700 nm, relatively strong Ar ⁺ lines for 400 < λ < 500 nm.
Life times (τ)	The relevant upper levels of N ₂ ⁺ have τ ≈ 60 ns. Cascades seem to play no role.	The relevant upper levels of Ne ⁺ have τ ≤ 10 ns, unknown cascade influence. The 2p ₁ Ne level has τ ≈ 15 ns, little cascade influence.	The relevant upper levels of Ar ⁺ have 10 < τ ≤ 20 ns, cascade influence might be relevant. Strong Argon lines have 20 ≤ τ ≤ 40 ns, cascades are relevant.
Mass	28 u	20 u	40 u
τ ² /m	129 ns ² /u	≤ 5 ns ² /u, if no cascades!	2.5 < τ ≤ 10 ns ² /u, if no cascades!
Exp. data availability for σ	Up to 1 keV for e ⁻ , up to 450 GeV for p.	Ne: up to 1 keV for e ⁻ , up to 1 MeV for p. Ne ⁺ : no data identified yet.	Ar: up to 250 eV for e ⁻ , none for p. Ar ⁺ : up to 250 eV for e ⁻ , none for p.
Photo-cathode efficiency	Good for the strongest N ₂ ⁺ lines.	Poor for main Ne lines, good for Ne ⁺ lines.	Very poor for main Ar lines, good for Ar ⁺ lines.
e.m. fields influence	Relatively strong distortion expected due to large τ ² /m	None for Ne, relatively low distortion expected for Ne ⁺ because of low τ ² /m	None for Ar, relatively low distortion expected for Ar ⁺ because of low τ ² /m
Integration time	Very low for e ⁻ , low for p, as estimated for the N ₂ ⁺ 391.4 nm line.	Low for e ⁻ , large for p, as estimated for the Ne 585.4 nm line.	Lower than for Ne but large as compared to N ₂ ⁺ . Integration over 400 < λ < 500 nm useful!

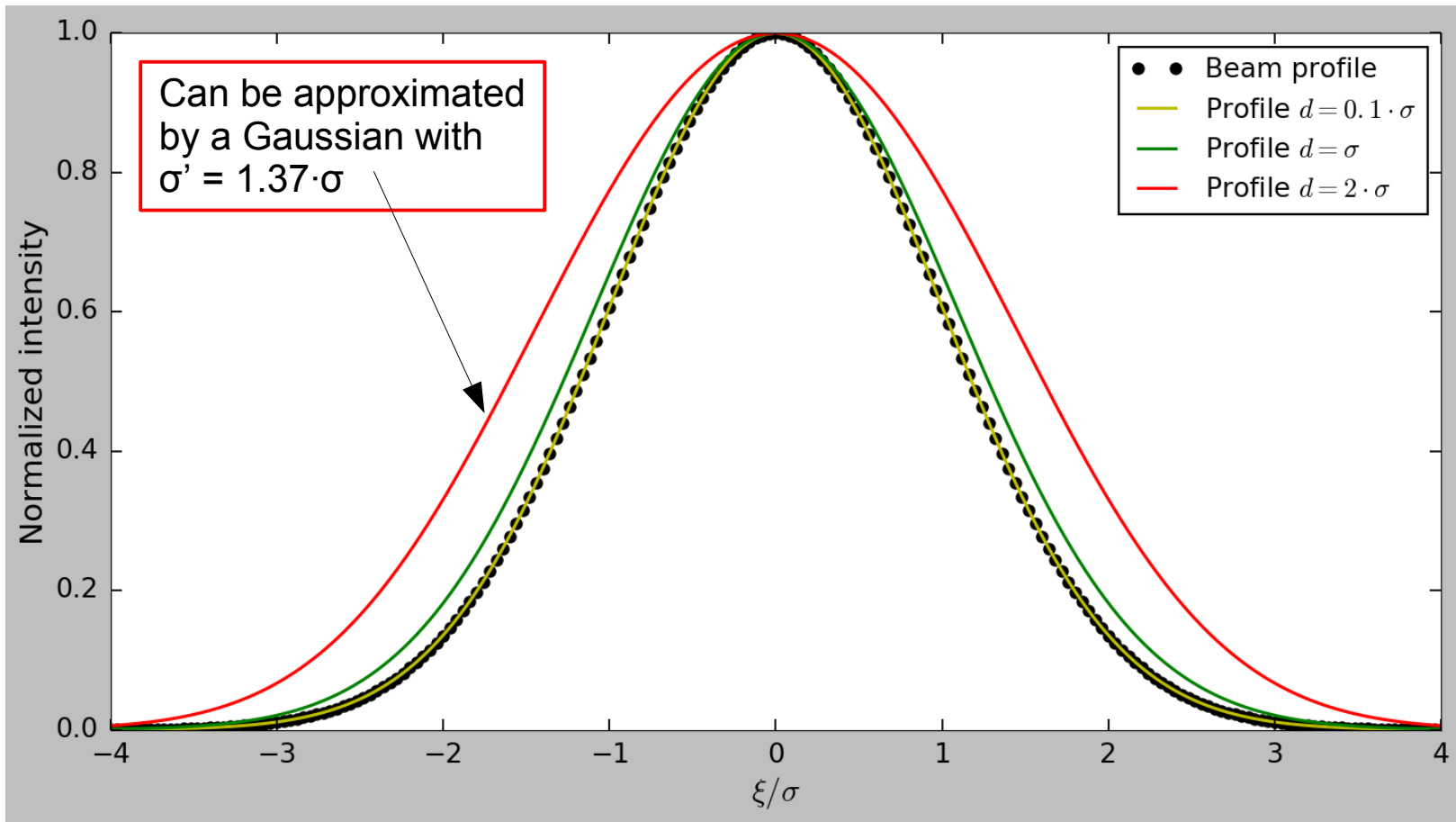
Influence of curtain thickness: Assumptions



- Gas curtain's density ρ depends only on y
- Gas curtain's refractive index is 1
- Gas curtain extends from $y = -d/2$ to $y = d/2$
- 1D detector parallel to the ξ axis
- Ideal optics placed practically at infinity
- Practically infinite depth of field
- $0 \leq \beta < 90^\circ$ (**presently 45°**)
- $-90^\circ < \alpha < 90^\circ$ (**presently 45°**)

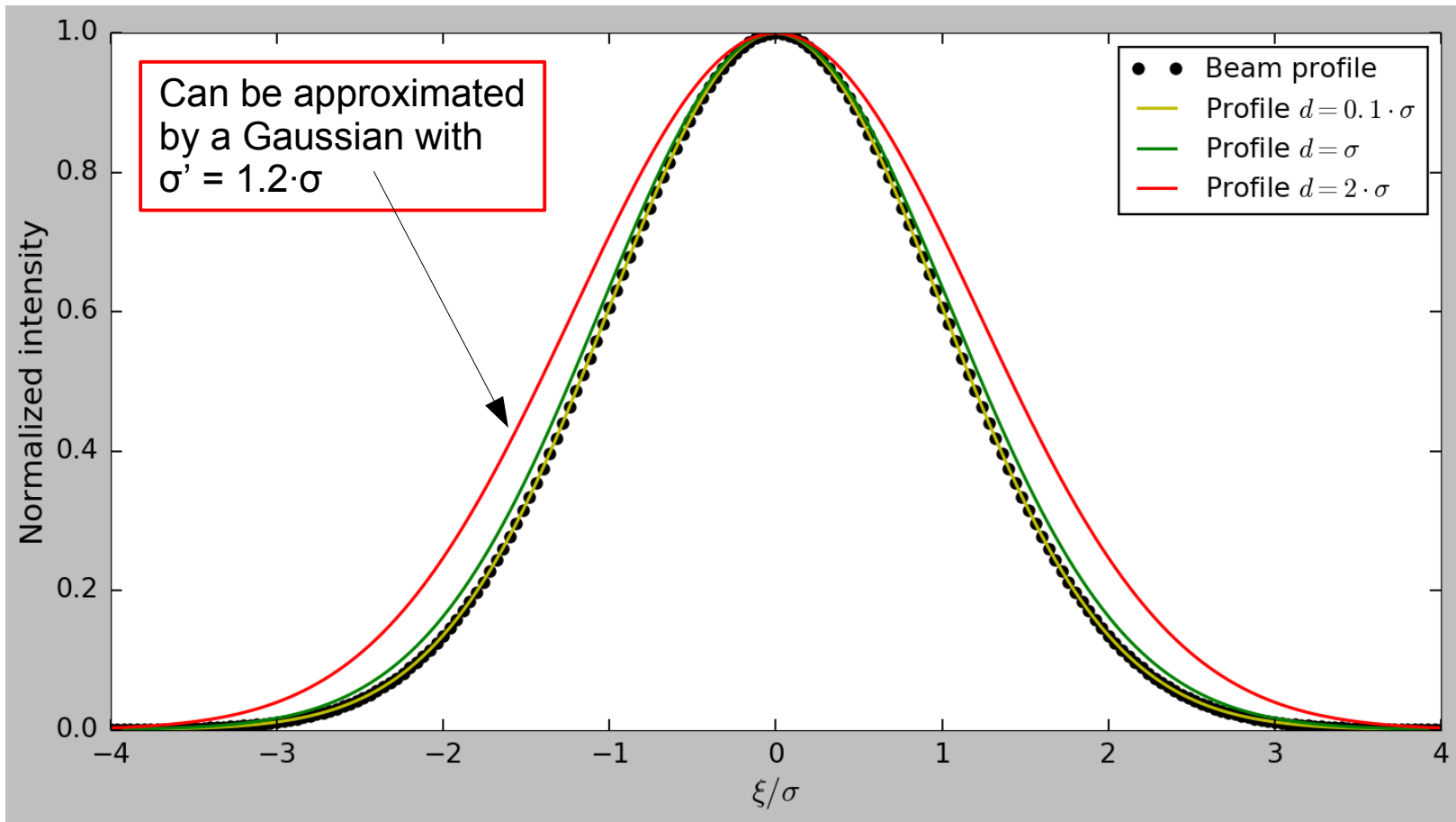
$$I(\xi) \propto \int_{-d/2}^{d/2} \rho(y) \cdot \phi\left(\xi \cdot \frac{\cos(\alpha)}{\cos(\beta)} - \frac{\sin(\alpha + \beta)}{\cos(\beta)} \cdot y\right) dy$$

Gaussian beam & homogeneous gas curtain



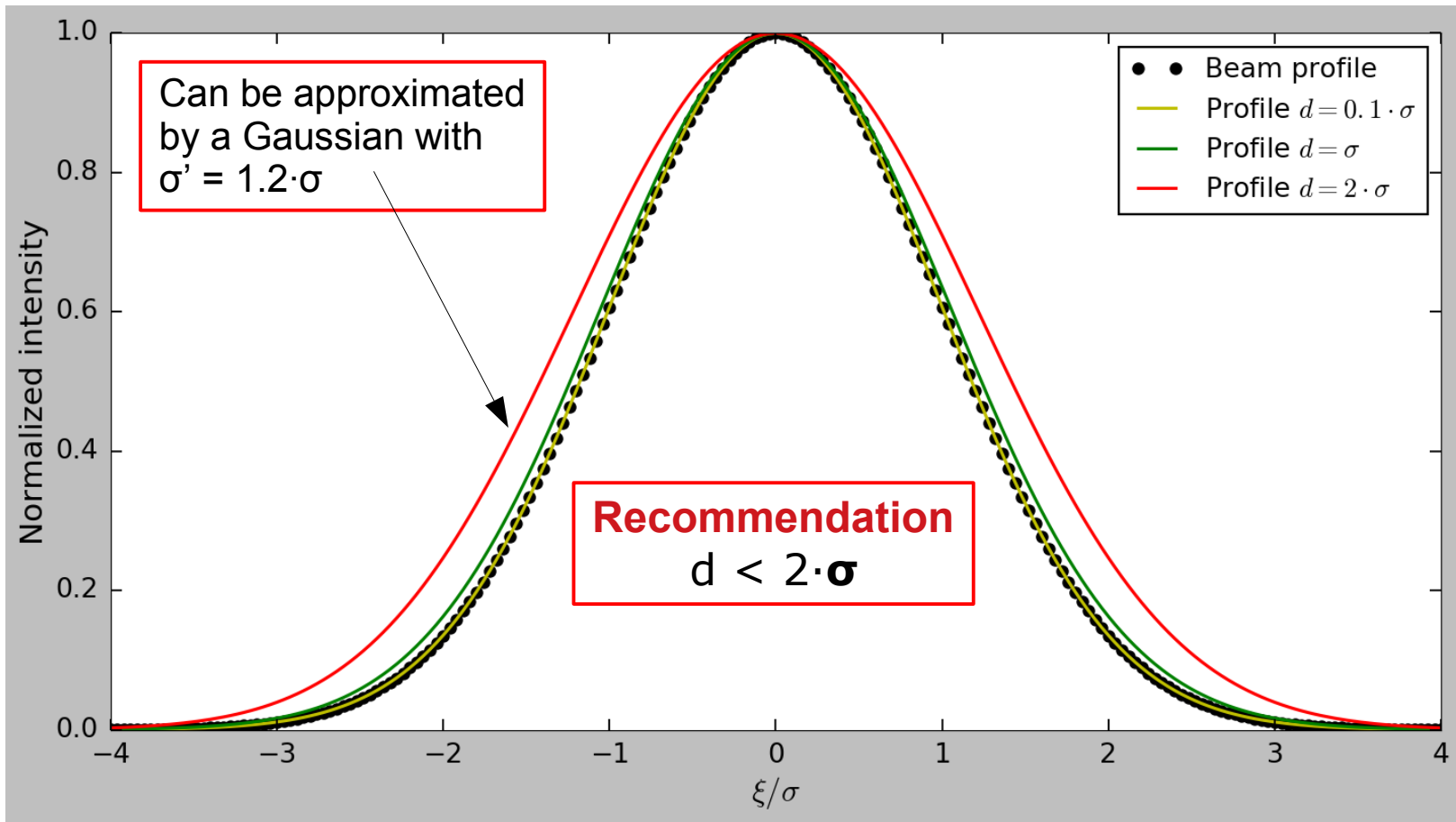
Line of sight and beam axis are perpendicular to each other, moreover $\alpha = \beta = 45^\circ$
The charged particle beam has a Gaussian profile with standard deviation σ , three gas curtain thicknesses d are considered: $0.1 \cdot \sigma$, σ and $2 \cdot \sigma$.

Gaussian beam & parabolic gas curtain profile



Line of sight and beam axis are perpendicular to each other, moreover $\alpha = \beta = 45^\circ$
The charged particle beam has a Gaussian profile with standard deviation σ , three gas curtain thicknesses d are considered: $0.1 \cdot \sigma$, σ and $2 \cdot \sigma$.

Gaussian beam & parabolic gas curtain profile



Line of sight and beam axis are perpendicular to each other, moreover $\alpha = \beta = 45^\circ$
The charged particle beam has a Gaussian profile with standard deviation σ , three gas curtain thicknesses d are considered: $0.1 \cdot \sigma$, σ and $2 \cdot \sigma$.

Possible show stoppers



- **secondary, low energy electrons and ions** accumulating in the e-lens may generate a strong background due to the usually high fluorescence cross sections at low energies
- **gas curtain density and thickness** since thin curtains are needed for good spatial resolution the gas density has to be maximized
- **strong electromagnetic fields** in case of ions as emitters
- **energy distribution of the electrons** within the main hollow beam since cross sections are energy dependent. For energies between 1 and 10 keV one may use the following power laws to estimate the cross sections: $5.4 \cdot 10^{-18} \cdot E^{-0.77}$ for N_2^+ , $1.5 \cdot 10^{-19} \cdot E^{-1.03}$ for Ne, $7.5 \cdot 10^{-19} \cdot E^{-0.43}$ for Ar and $7.4 \cdot 10^{-20} \cdot E^{-0.79}$ for Ar^+ , $[\sigma] = \text{cm}^2$, $[E] = \text{keV}$



There is no clear winner yet, but Ne emitting at 584.5 nm might be finally the best choice, especially if a detector (camera) can be identified which has good – at least 20% – efficiency at this wavelength and is capable of single photon detection.

An alternative technical solution may be an emCCD camera, classical or back illuminated.